Effect of Cations in Infrared and Computational Analysis of Vanadium-Containing Six-Coordinate Oxotungstates

Olga Dmitrenko,[†] Wenlin Huang,[‡] Tatyana E. Polenova,[†] Lynn C. Francesconi,[‡] James A. Wingrave,[†] and Andrew V. Teplyakov*[,†]

Department of Chemistry and Biochemistry, University of Delaware, Newark, Delaware 19716, and Department of Chemistry of the City University of New York & the Graduate School, Hunter College, New York, New York 10021

Received: December 9, 2002; In Final Form: March 26, 2003

Complex salts of $VW_5O_{19}^{3-}$, *cis*-$V_2W_4O_{19}$,$^{4-}$, and $W_6O_{19}^{2-}$ anions have been investigated using Fourier transform infrared spectroscopy and density functional theory computational methods. The intensities of the infrared absorption bands commonly used to identify the bridge and terminal oxygen atoms in these hexametalate systems were found to depend drastically on the nature of the countercation and presence of water in the salts. Theoretical investigations suggest that the anions alone may not show significant absorption in the region commonly assigned to the M−O_t vibrations (subscripts t and b denote terminal and bridged oxygen atoms, respectively). At the same time, the addition of even a single molecule of water or tetraalkylammonium into the calculation results in almost quantitative agreement between the theoretical and experimental spectra. The presence of vanadium has a profound effect both on M−O_t and on M−O_b−M vibrations.

Introduction

Polyoxometalates are a versatile class of inorganic compounds. Such characteristics as tunability of size and charge, inclusion of a variety of transition metals and main group elements made them very valuable in catalysis and materials science. Polyoxometalate chemistry is a mature field. Nevertheless, interest in this subject keeps increasing, as evidenced by numerous reviews[1−3] and references therein. Polyoxometalates (POMs) present almost perfect models for structural and electronic analysis of starting materials for many industrial processes. POMs have found many applications encompassing oxidation catalysts, corrosion-resistant coatings, dyes and pigments, additives and dopants, precursors to mixed oxide films, membranes, and sensors (see review[3] and references therein). They also exhibit unusual photo- and electrochromic properties.[4−7]

Vibrational methods have often been used for quick and reliable characterization of the structures of polyoxometalates.[8−11] Compounds synthesized in a laboratory environment as well as industrial catalysts can be characterized within minutes using infrared spectroscopy. Although vibrational analysis may not give complete structural information, it provides key spectral assignments that can be used to deduce the structural and often electronic properties of polyoxometalates. The vibrational features of the Lindqvist-type and similar structures have been originally assigned on the basis of two drastically different positions of oxygen in these systems: the bridge (M−O_b−M) and the terminal (M−O_t).[12−16] Sometimes, structural information can be obtained by careful analysis of these and other absorption bands. For example, corner-sharing and edge-sharing octahedra in some polyoxometalates of the so-called Keggin structure have been assigned.[16] A good agreement with the structural and vibrational experimental data has also been demonstrated using density functional calculations (DFT) for *isolated* $[M_6O_{19}]^{n-}$ anions of Lindqvist structure.[17−19] Even though the effects of stabilization by the surrounding media were neglected in those studies, the authors reported that the experimental data for polyanions containing Mo and W were reproduced quite well.

Model studies outlined in this paper examine the effects of the surrounding media on the structure and the vibrational spectra of polyanions. In fact, the influence of counterions has been documented experimentally in both assembly/structure of polyoxometalates and in their catalytic activities.[20−25] Here, one of the simplest polyoxometalates, the six-coordinate Lindqvist anion, is considered. Extensive structural and spectroscopic characterization of this type of polyoxometalates makes them excellent benchmark systems for the studies discussed herein.[8,9,26−29] The changes in the vibrational band structure of hexatungstate anions are probed as a function of the counterion and the presence of water in the salt. The effects of replacing one or two tungsten atoms with vanadium are also described. In addition to changing the symmetry of the molecule under investigation, vanadium significantly affects the electronic properties of hexametalates. It also has a profound influence on the coordination of commonly used counterions (such as tetraalkylammonium) and of water.

Since mixed V−W−O systems are often applied as oxidation catalysts, it is important to understand the electronic properties of these systems. The hexametalates analyzed here present a unique opportunity to model these electronic properties and to understand their significance in terms of possible catalytic processes. In this report, we demonstrate that the vibrational signatures of the hexametalates can potentially serve as benchmarks in designing materials with tunable structural and electronic properties for multiple applications.

* Corresponding author. Tel.: (302) 831-1969. Fax: (302) 831-6335. E-mail: andrewt@udel.edu.
[†] University of Delaware.
[‡] Hunter College.

10.1021/jp022560l CCC: $25.00
Published on Web 07/04/2003

Methods

Synthesis of Polyoxometalates. All the compounds discussed here were synthesized according to the literature protocols.[30] Elemental analysis and X-ray crystallographic characterization of the compounds obtained were performed at Hunter College and are discussed in detail elsewhere.[31]

Spectroscopic Methods. Experiments were performed using a Nicolet Magna 560 FTIR spectrometer with a liquid nitrogen cooled MCT detector. Standard KBr pellet preparation techniques were used. The pellets were prepared by careful mixing of the appropriate amounts of polyoxometalates to produce approximately 1% weight mixture, with KBr (Fluka, for IR spectroscopy). The pellets were obtained by applying 40 ft-lb to the screw of a 3/8-in. pellet press to produce a pellet of approximately 0.010-in. thickness as measured by a micrometer. Special precaution was taken to ensure that the infrared beam of the spectrometer had a diameter smaller than the 3/8-in. opening of the pellet press. Infrared spectra were recorded at room temperature with 4 cm^{-1} resolution and at least 32 scans per experiment. The absorption spectra were obtained by dividing the single-beam spectra of KBr pellets containing polyoxometalates by a single-beam spectrum of pure KBr, keeping all the other parameters the same throughout the course of the studies.

Computational Methods. Molecular orbital calculations using density functional theory (DFT) methods[32] were performed with the Gaussian 98 package.[33] The Becke three-parameter hybrid functional,[34,35] combined with the Lee, Yang, and Parr (LYP) correlation functional,[36] denoted B3LYP,[37] was employed in the calculations. Geometries were optimized[38−40] without any symmetry constraints with the analytical gradient using the LANL2MB basis set.[41−43] The LANL2DZ basis set has also been used for the naked ions. $[V_2W_4O_{19}]^{4-}$ has been re-optimized using the LANL2DZ basis set for V and W atoms, and 6-311+G(d,p) for oxygen atoms. In LANL basis sets developed for atoms of high atomic number, the core basis functions were replaced by an effective core potential (ECP). The more recent version, LANL2, retains some of the outer-core functions when applied to third- and higher-period atoms. The LANL basis sets are available either as a minimum (MB) or a double-ζ (DZ) basis. In LANL2MB and LANL2DZ, for first row atoms, Gaussian 98 utilizes STO-3G and D95, respectively. The optimized geometries are in general agreement with each other and with available experimental data.[27,31] Comparison of the B3LYP geometries of $[W_6O_{19}]^{2-}$ obtained with LANL2MB and LANL2DZ indicates only small structural differences ($W-O_c$ is 2.37 vs 2.38 Å, $W-O_b$ is 1.93 vs 1.94 Å, and $W-O_t$ is 1.74 in both cases). We also analyzed the geometries of $[V_2W_4O_{19}]^{4-}$ optimized with three basis sets of theory and compared them with the X-ray structures (see Table S2 in Supporting Information) and found no significant improvement with an extended basis set.

We were unable to perform calculations with the more extended LANL2DZ basis set for complexes of ions with water molecules or TMA because of significant CPU time requirements for systems of this size. In contrast to previous DFT studies,[18,19] here we do not use symmetry constraint, which also adds significantly to CPU-expense.

Harmonic vibrational frequencies were calculated analytically for each optimized structure. The B3LYP/LANL2DZ frequencies for naked ions are quite similar to those calculated with B3LYP/LANL2MB except for $W(V)-O_t$ vibrations which are about 1.1-fold larger and approximately twice more intense than corresponding B3LYP/LANL2MB vibrations (for example, $V-O_t$ stretch vibrations are 1186 vs 1069 cm^{-1}, see complete list of frequencies in Supporting Information). This does not affect qualitative conclusions based upon B3LYP/LANL2MB calculations.

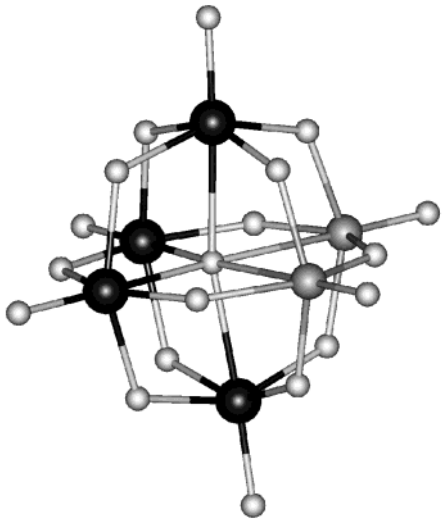

Figure 1. Schematic diagram of a hexametalate anion (Lindqvist structure).

The B3LYP/LANL2MB harmonic frequencies have been scaled by 0.97, which is consistent with scaling factors reported for the B3LYP method.[44,45]

Results and Discussion

Six-coordinated oxometalates of the Lindqvist structure were the primary species studied here. A schematic representation of a generalized Lindqvist structure is given in Figure 1. Figure 2 compares the experimental infrared spectrum of the $[W_6O_{19}]^{4-}$ anion stabilized by tetrabutylammonium ($(TBA)_2W_6O_{19}$), and the theoretically predicted vibrational spectra of the free $[W_6O_{19}]^{4-}$ anion, the same anion with a water molecule bound to its terminal oxygen atom and to its bridged oxygen atom, and the $[W_6O_{19}]^{4-}$ anion stabilized with one tetramethylammonium cation. The corresponding energy-minimized structures are presented in Figure 3 (structures **Ia**−**Ic**). The spectrum in Figure 2a is in agreement with the hexatungstate infrared signatures observed previously.[27,29] Frequency simulations for the bare $[W_6O_{19}]^{2-}$ anion, **I**, suggest that the major components of the characteristic groups of absorption bands are quite predictable. Three groups of the vibrations can be allocated: terminal O_t-W stretch vibrations in their different combinations (experimental peak at 974 cm^{-1}), bridged $W-O_b-W$ stretch vibrations in their different combinations (experimental peak at 812 cm^{-1}), and $W-O_b-W$ bending vibration combinations (low-intensity bands located around 588 cm^{-1}). Similar groups of vibrations will be described below for $[VW_5O_{19}]^{3-}$ and $[V_2W_4O_{19}]^{4-}$ systems.

To understand the effects of environment on the infrared spectra of $[W_6O_{19}]^{2-}$ anions, the model hydrogen-bonded molecular complexes (with water and tetramethylammonium (TMA) interacting with terminal and bridged oxygen atoms) were optimized, as shown in Figure 3 (structures **Ia**−**Ic**). The corresponding calculated IR spectra are given in Figure 2. The predicted spectrum of a model $(TMA)[W_6O_{19}]^{1-}$ anion (Figure 2f) is in good qualitative agreement with the experimental spectrum of $(TBA)_2[W_6O_{19}]$. In the model complex, the TMA cation is interacting with three oxygen atoms via strong $C-H\cdots O$ hydrogen bonds ($|C-O|$ distances are ca. 2.8 Å). According to

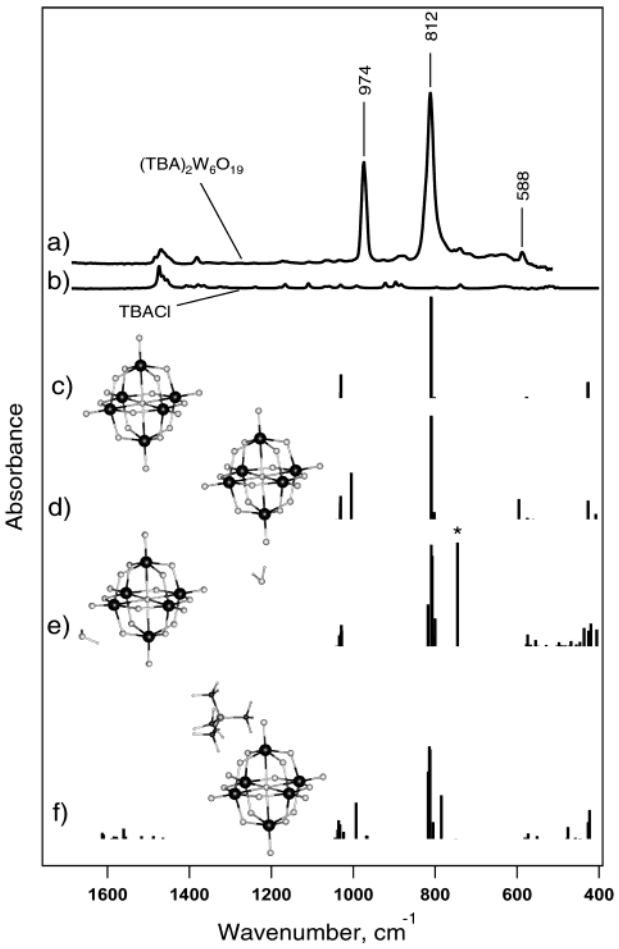

Figure 2. Infrared spectroscopic studies of (a) $(TBA)_2W_6O_{19}$ in a KBr pellet compared to the spectrum of (TBA)Cl (b) obtained by the same technique. The theoretical prediction of the vibrational frequencies for (c) a $[W_6O_{19}]^{2-}$ anion, **I**; (d) same anion with one water molecule in a terminal oxygen position, **Ic**; (e) a water molecule on a bridge oxygen position, **Ib**; and (f) stabilized by one tetramethylammonium cation, **Ia**, are compared. Scaling factor of 0.97 was used to fit experimental data.

our calculations, these hydrogen bonds lead to a significant shift of the active terminal O_t-W stretch vibration and its intensity increases (note, that other O_t-W stretch vibrations not involved in the hydrogen bonding are not shifted). The interaction of the TMA cation with the bridged oxygen atoms causes splitting of the $W-O_b-W$ stretch vibrations.

Inclusion of a single water molecule provides an excellent tool for understanding the sensitivity of particular vibrational modes of the hexametalate anions toward the presence of water. Comparing the results for bridged and terminally attached water molecules, as illustrated in Figure 2 d−e, it would appear that terminal water affects mainly terminal O_t-W vibrations, whereas water that is hydrogen-bonded to the bridged oxygen atom splits bridged $W-O_b-W$ stretch vibrations resulting in a broadening of the corresponding absorption band observed experimentally. The new intense absorption band at 769 cm^{-1} (unscaled, marked with an asterisk in Figure 2e) represents the vibration of the water hydrogen atom, hydrogen-bonded to the oxygen of the $W-O_b-W$ bridge toward the closest W atom. This mode was not observed in the case of $(TMA)[W_6O_{19}]^{1-}$. Comparison of the total energies of structures **Ib** and **Ic** (Figure 3) points toward the increased stability of the water molecule on the oxygen bridge site by approximately 8 kcal/mol, as compared to the terminal site.

If one tungsten atom is replaced by a vanadium in the Lindqvist structure (**II**, Figure 3), the most intense absorption band of $W-O_b-W(V)$ stretch vibrations (experimental peak is at 802 cm^{-1}) broadens significantly, as shown in Figure 4a (infrared spectrum of (TBA)Cl is given for comparison in Figure 4b). The experimental spectrum of $[VW_5O_{19}]^{3-}$ was measured with the TBA cation and shows the $W-O_t$ vibrations markedly shifted, as compared with $[W_6O_{19}]^{2-}$ (953 vs 974 cm^{-1}), and with single satellite $V-O_t$ vibrations peaked at 989 cm^{-1}. Now the $M-O_t$ vibrations include both $W-O_t$ and $V-O_t$, while bridge vibrations include $W-O_b-W$ and $W-O_b-V$. Interestingly, the absorption bands corresponding to the terminal oxygen cannot be reproduced theoretically unless the tetramethylammonium cation is included in the calculations, as evidenced by plots c, d, and e in Figure 4. Thus, it is clear that the molecular motions associated with the terminal oxygen atoms of the Lindqvist structure are affected profoundly by hydrogen bonding.

In the simulated $(TMA)[VW_5O_{19}]^{2-}$ spectrum in Figure 4d, the $V-O_t$ stretch vibration (unscaled frequency is 1197 cm^{-1}) does not exhibit any significant shift as expected, since TMA is attached to the side of the hexametalate structure opposite to the vanadium atom location. Obviously, the more complete model with at least three TMA cations surrounding the $[VW_5O_{19}]^{3-}$ cluster would describe the experimental spectrum in a much more realistic way. Currently, such a large calculation is not feasible because of intensive computational demands. However, the attempt to put the TMA molecule on the other side of the $[VW_5O_{19}]^{2-}$ anion (close to the vanadium atom) results in a spectrum shown in Figure 4e that is less similar to the experimental data than the spectrum in Figure 4d. Nevertheless, it predicts the tendency (intensity increase and red-shift) for the $V-O_t$ stretch vibration changes induced by hydrogen bonding.

The replacement of one W atom by a V atom in $[W_6O_{19}]^{2-}$ to obtain $[VW_5O_{19}]^{3-}$ increases the net negative charge of the hexametalate anion from −2 to −3 which should affect the strength of the hydrogen-bonding interactions.[46] Thus, one may expect more pronounced characteristic spectral changes as the number of vanadium atoms in a six-coordinated oxotungstate anion system increases. The larger shifts of the terminal $W-O_t$ and $V-O_t$ stretch vibrations can be attributed to the stronger hydrogen-bonding interactions.

When two atoms of tungsten are substituted by vanadium in a $[W_6O_{19}]^{2-}$ anion, the formal symmetry of the Lindqvist structure is further broken to produce a $[V_2W_4O_{19}]^{4-}$ anion, **III**. The effects of this cis substitution,[26] as well as the effects of the water presence in the polyoxometalate salt, are examined in Figures 5 and 6, which summarize the experimental and theoretical studies involving $(TBA)_4[V_2W_4O_{19}]$ (the infrared spectrum of (TBA)Cl is given in Figure 5b and a predicted spectrum of a bare anion is given in Figures 5e and 6e for reference) and $Na_2(Cs)_2[V_2W_4O_{19}]\cdot 2H_2O$. The infrared spectrum in Figure 5a is reproduced quite well by a model with one TMA^+ cation, **IIIa**, when a scaling factor of 0.99 is used. A somewhat less similar spectrum is produced if the TMA molecule is located on the side of the anion with two vanadium atoms, **IIIe**, as shown in Figure 5d. In the experimental vibrational spectrum of $Na_2(Cs)_2[V_2W_4O_{19}]$ in Figure 6a, the presence of water is clearly observed on the basis of the O−H stretching region (around 3300 cm^{-1}, not shown). The fine vibrational structure that is easily resolved in Figure 5a essentially disappears when the water is present in the sample under analysis. Although the overall spectra are quite similar,

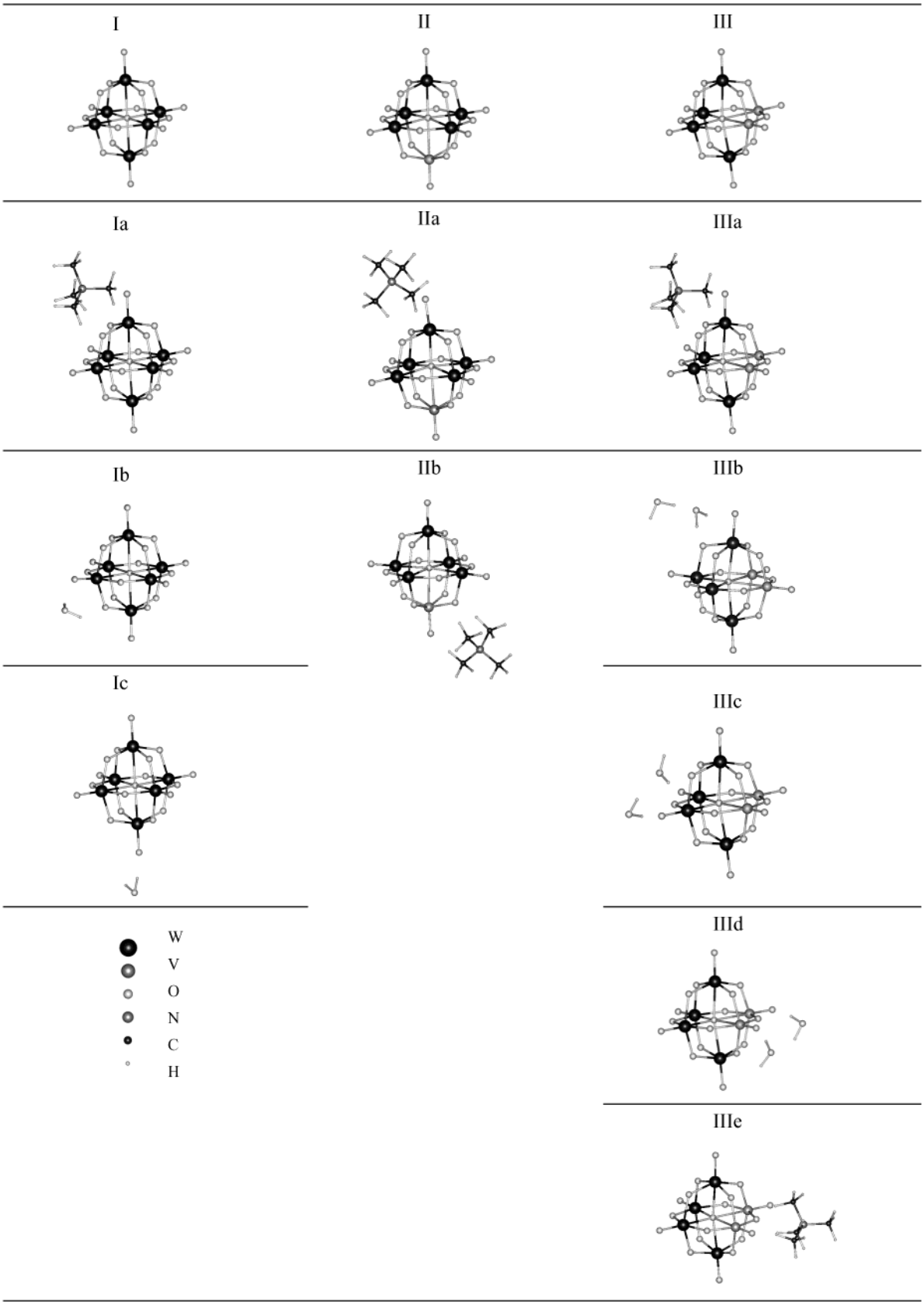

Figure 3. Energy-minimized structures predicted for $[W_6O_{19}]$,$^{4-}$ $[VW_5O_{19}]^{3-}$, and $[V_2W_4O_{19}]^{4-}$ anions interacting with water and tetramethylammonium (TMA) cation.

the broad feature at 785 cm^{-1} observed for $Na_2(Cs)_2[V_2W_4O_{19}]$ splits into two bands at 750 and 804 cm^{-1} corresponding to the vibrational motion involving mainly bridge oxygen atoms for $(TBA)_4[V_2W_4O_{19}]$. The 974 cm^{-1} feature in Figure 6a with a shoulder around 994 cm^{-1} splits into a set of absorption features at 991, 974, and 947 cm^{-1}. The models presented in Figure 6 include the bare $[V_2W_4O_{19}]^{4-}$ anion, **III**; the same anion with the water molecule adsorbed on a bridge site, and another water

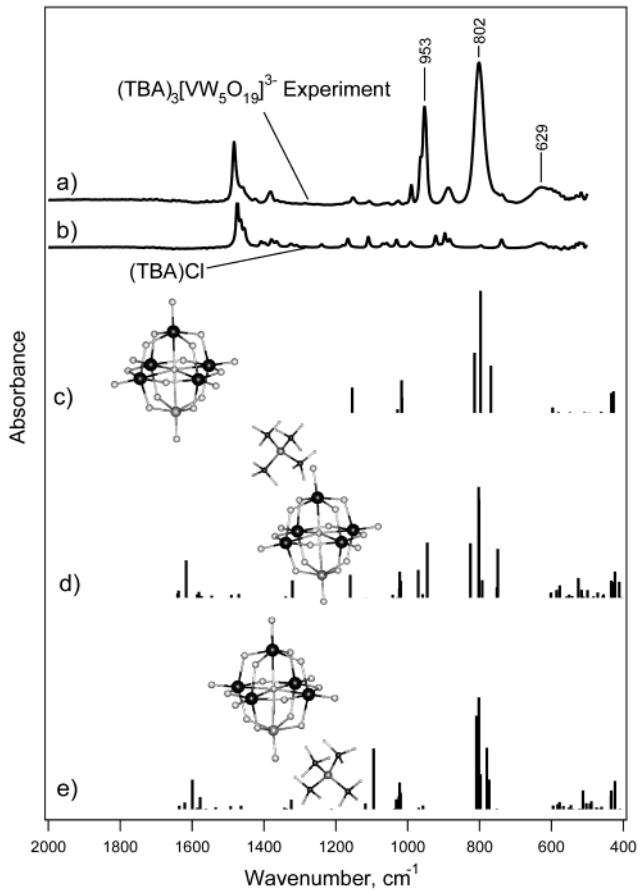

Figure 4. Infrared spectroscopic studies of (a) $(TBA)_3[VW_5O_{19}]$ in a KBr pellet and (b) TBACl in a KBr pellet compared to (c) theoretically predicted IR spectrum of $[VW_5O_{19}]^{3-}$, **II**; (d) theoretically predicted IR spectrum of $(TMA)[VW_5O_{19}]^{2-}$, **IIa**; and (e) theoretically predicted IR spectrum of $(TMA)[VW_5O_{19}]^{2-}$, **IIb**, where the TMA molecule is located near the vanadium atom. A scaling factor of 0.97 was used to fit experimental data.

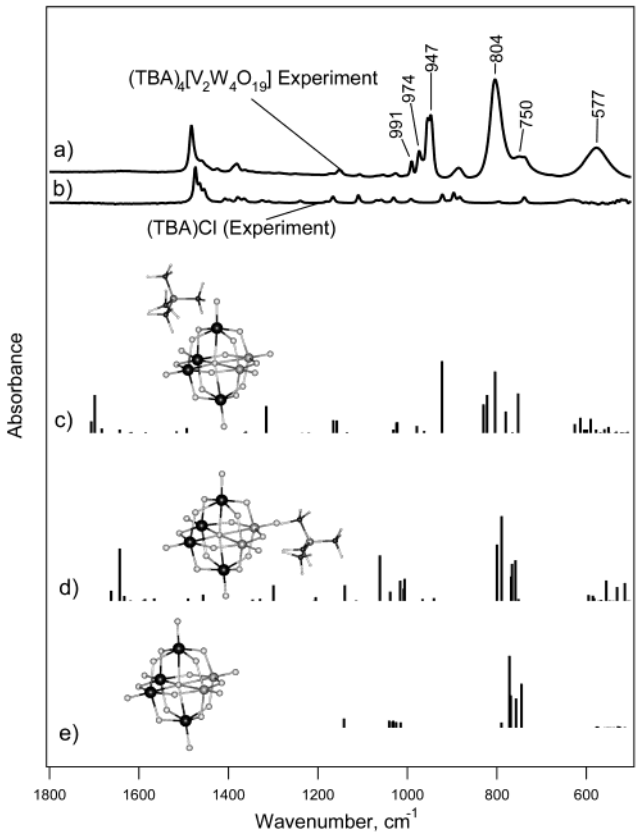

Figure 5. Infrared spectroscopic studies of (a) $(TBA)_4[V_2W_4O_{19}]$ in a KBr pellet and (b) (TBA)Cl in a KBr pellet compared with (c) theoretically predicted IR spectrum of $(TMA)[V_2W_4O_{19}]^{3-}$, **IIIa**, and (d) theoretically predicted IR spectrum of $(TMA)[V_2W_4O_{19}]^{3-}$, **IIIe**, where the TMA molecule is located near the vanadium atoms; and (e) bare $[V_2W_4O_{19}]^{2-}$ anion, **III**. A scaling factor of 0.99 was used to fit experimental data.

molecule hydrogen-bonded to the first water molecule, **IIIb**; the $[V_2W_4O_{19}]^{4-}$ anion with two water molecules bound at the terminal oxygen atoms as shown in scheme **IIIc** of Figure 3; and the $[V_2W_4O_{19}]^{4-}$ anion with two water molecules bound at the terminal oxygen atoms as shown in scheme **IIId** of Figure 3. As evidenced by this comparison, the presence of hydrogen bonds provided by either a water molecule or a TMA^+ cation is essential for the satisfactory computational analysis of the experimental infrared data. According to the calculations, we may assign the 974 cm^{-1} band to the terminal $W-O_t$ stretch. Bands at 991 and 974 cm^{-1} can be assigned to in-phase and out-of phase combinations of $V-O_t$ stretches shifted by hydrogen-bonding interactions from their "gas-phase" positions.

In addition to the presence of the intense absorption modes corresponding to the terminal oxygen atoms, the lower-intensity 750 cm^{-1} band, which is only observed for vanadium-containing compounds, is reproduced for $(TBA)_4[V_2W_4O_{19}]$ (where it is resolved from the main 804 cm^{-1} peak) and for $Na_2(Cs)_2[V_2W_4O_{19}]$ (where it is only present as an unresolved shoulder as a result of strong hydrogen-bonding with multiple water molecules).

Both homogeneous and inhomogeneous broadening is likely to play a role in the differences between $Na_2(Cs)_2[V_2W_4O_{19}]$ and $(TBA)_4[V_2W_4O_{19}]$. When a $[V_2W_4O_{19}]^{4-}$ anion is modeled without any water molecules present, the group of vibrational bands centered around 785 cm^{-1} is reproduced reasonably well. However, the other group of vibrations involving terminal oxygen atoms in the hexametalate anion is basically not observed. On the other hand, if two molecules of water are included into the theoretical model (as in species **IIIc** shown in Figure 3), the infrared spectrum in Figure 6a is reproduced nearly quantitatively. Terminal water adsorption not only shifts $O_t-W(V)$ vibrations but also increases their intensity.

The inhomogeneous broadening of both main groups of absorption bands is apparently caused by several factors. The inclusion of vanadium into the hexametalate frame causes a series of complex vibrations involving bridge oxygen atom absorption bands to split into an even more complex series, where the exact position of the absorption bands depends on the structure of the salt. It has been shown that $(TBA)_4[V_2W_4O_{19}]$ crystallizes in a c_2/c space group with one anion per unit cell.[31] The $[V_2W_4O_{19}]^{4-}$ anions are located at the corners; however, each individual $[V_2W_4O_{19}]^{4-}$ anion assumes a different orientation. Moreover, positional disorder is present in the structure with respect to the vanadium atoms.[31] In addition, the inclusion of water enhances the intensity of the group of vibrations around 990 cm^{-1} with the simple motion of terminal $M-O_t$ as the major component. Although the inclusion of additional water molecules may add to the complexity of the theoretically predicted spectrum because of the inhomogeneous broadening of the absorption bands, it is unlikely that any new significant qualitative or quantitative differences will be acquired.

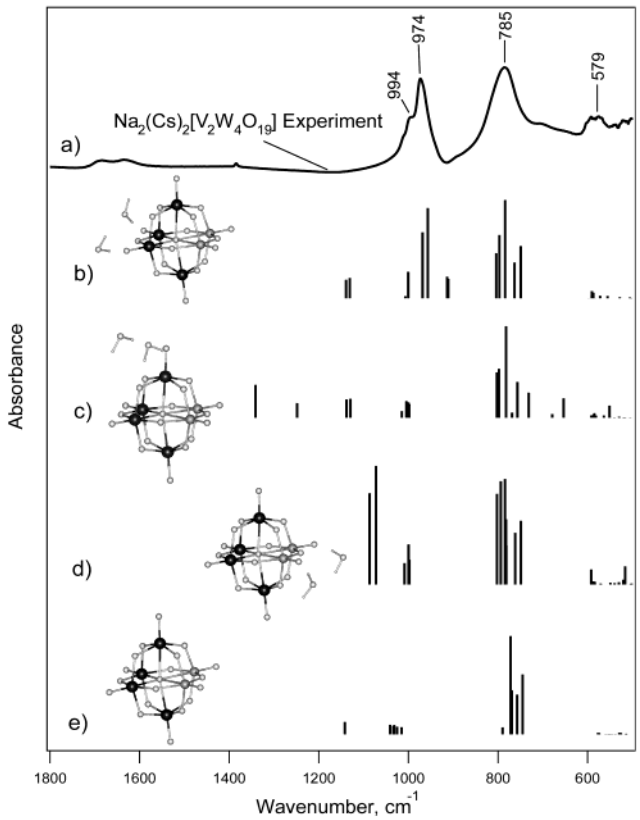

Figure 6. Infrared spectroscopic studies of the effect of the water on the infrared spectra of hexametalate anions is shown for (a) $Na_2(Cs)_2[V_2W_4O_{19}]\cdot 2H_2O$ in a KBr pellet as compared to the theoretical prediction of the vibrational frequencies of (b) the $[V_2W_4O_{19}]^{2-}$ anion with two molecules of water on terminal oxygen atoms, **IIIc**; (c) the same anion with two molecules of water attached sequentially at the bridge position, **IIIb**; (d) same anion with two molecules of water on terminal oxygen atoms as shown in scheme **IIId** of Figure 3; and (e) bare $[V_2W_4O_{19}]^{2-}$ anion, **III**. A scaling factor of 0.97 was used to fit experimental data.

Conclusions

Six-coordinate vanadium-substituted oxotungstates with Lindqvist structure have been studied using infrared spectroscopy and DFT calculations. It was shown that the vibrational spectra can be reproduced theoretically and that the inclusion of organic cation, and water molecules has a profound effect on the vibrational spectra. In addition, it was demonstrated that two major groups of vibrational features originally assigned to terminal and bridged oxygen atoms in these structures are actually groups of more complex atomic motions.

Acknowledgment. O.D. was supported by the National Science Foundation (CHE-0138632). We are also thankful to the National Center for Supercomputing Applications, Urbana, Illinois, and Lexington, Kentucky, for generous amounts of computer time.

Supporting Information Available: Total energies, Cartesian coordinates, IR frequencies, and charge distribution. This material is available free of charge via the Internet at http://pubs.acs.org.

References and Notes

(1) Pope, M. T.; Müller, A. *Angew. Chem., Int. Ed. Engl.* **1991**, *30*, 34−48.

(2) Coronado, E.; Gómez-Garcia, C. J. *Chem. Rev.* **1998**, *98*, 273−296.

(3) Katsoulis, D. E. *Chem. Rev.* **1998**, *98*, 359−387.

(4) Gomez-Romero, P. *Adv. Mater.* **2001**, *13*, 307−325.

(5) Yamase, T. *Chem. Rev.* **1998**, *98*, 307−325.

(6) Liu, S.; Kurth, D. G.; Möhwald, H.; Volkmer, D. *Adv. Mater.* **2002**, *14*, 225−228.

(7) Liu, S.; Kurth, D. G.; Bredenkötter, B.; Volkmer, D. *J. Am. Chem. Soc.* **2002**, *124*, 12279−12287.

(8) Flynn, C. M., Jr.; Pope, M. T. *Inorg. Chem.* **1971**, *10*, 2524−2529.

(9) Flynn, C. M., Jr.; Pope, M. T. *Inorg. Chem.* **1971**, *10*, 2745−2750.

(10) Flynn, C. M., Jr.; Pope, M. T. *Inorg. Chem.* **1972**, *11*, 1950−1952.

(11) Nomiya, K.; Nozaki, C.; Miyazawa, K.; Shimizu, Y.; Takayama, T.; Nomura, K. *Bull. Chem. Soc. Jpn.* **1997**, *70*, 1369−1377.

(12) Ferrer, E. G.; Baran, E. J. *Biol. Trace Elem. Res.* **2001**, *83*, 111−119.

(13) Villaneau, R.; Proust, A.; Robert, F.; Gouzerh, P. **1999**.

(14) Briand, L. E.; Thomas, H. J.; Baronetti, G. T. *Appl. Catal. A* **2000**, *201*, 191−202.

(15) Wu, Q.; Tao, S.; Lin, H.; Meng, G. *Mater. Sci. Eng.* **2000**, *B68*, 161−165.

(16) Béreau, V.; Cadot, E.; Bögge, H.; Müller, A.; Sécheresse, F. *Inorg. Chem.* **1999**, *38*, 5803−5808.

(17) Bridgeman, A. J.; Cavigliasso, G. *Inorg. Chem.* **2002**, *41*, 1761−1770.

(18) Bridgeman, A. J.; Cavigliasso, G. *Chem. Phys.* **2002**, *279*, 143−159.

(19) Li, J. *J. Clust. Sci.* **2002**, *13*, 137−163.

(20) Kirby, J. F.; Baker, L. C. W. *Inorg. Chem.* **1998**, *37*, 5537−5543.

(21) Kim, K.-C.; Pope, M. T. *J. Am. Chem. Soc.* **1999**, *121*, 8512−8517.

(22) Grigoriev, V. A.; Hill, C. T.; Weinstock, I. A. *J. Am. Chem. Soc.* **2000**, *122*, 3544−3545.

(23) Grigoriev, V. A.; Cheng, D.; Hill, C. L.; Weinstock, I. A. *J. Am. Chem. Soc.* **2001**, *123*, 5292−5307.

(24) Johnson, B. J. S.; Schroden, R. C.; Zhu, C.; Stein, A. *Inorg. Chem.* **2001**, *40*, 5972−5978.

(25) Johnson, B. J. S.; Schroden, R. C.; Zhu, C.; Vivtor, G.; Young, J.; Stein, A. *Inorg. Chem.* **2002**, *41*, 2213−2218.

(26) Klemperer, W. G.; Shum, W. *J. Am. Chem. Soc.* **1978**, *100*, 4891−4893.

(27) Fuchs, J. *Z. Naturforsch.* **1973**, *28b*, 389−404.

(28) Fuchs, v. J.; Freiwald, W.; Hartl, H. *Acta Crystallogr.* **1978**, *B34*, 1764−1770.

(29) Mattes, v. R.; Bierbüsse, H.; Fuchs, J. *Z. Anorg. Allg. Chem.* **1971**, *385*, 230−242.

(30) Domaille, P. J. *J. Am. Chem. Soc.* **1984**, *106*, 7677−7687.

(31) Huang, W.; Todaro, L.; Francesconi, L. C.; Polenova, T. E. *J. Am. Chem. Soc.* **2003**, *125* (19), 5928−5938.

(32) Hehre, W. J.; Radom, L.; Schleyer, P. v. R.; Pople, J. A. *Ab Initio Molecular Orbital Theory*; Wiley: New York, 1986.

(33) Frisch, M. J.; Trucks, G. W.; Schlegel, H. B.; Scuseria, G. E.; Robb, M. A.; Cheeseman, J. R.; Zakrzewski, V. G.; Montgomery, J. A., Jr.; Stratmann, R. E.; Burant, J. C.; Dapprich, S.; Millam, J. M.; Daniels, A. D.; Kudin, K. N.; Strain, M. C.; Farkas, O.; Tomasi, J.; Barone, V.; Cossi, M.; Cammi, R.; Mennucci, B.; Pomelli, C.; Adamo, C.; Clifford, S.; Ochterski, J.; Petersson, G. A.; Ayala, P. Y.; Cui, Q.; Morokuma, K.; Malick, D. K.; Rabuck, A. D.; Raghavachari, K.; Foresman, J. B.; Cioslowski, J.; Ortiz, J. V.; Stefanov, B. B.; Liu, G.; Liashenko, A.; Piskorz, P.; Komaromi, I.; Gomperts, R.; Martin, R. L.; Fox, D. J.; Keith, T.; Al-Laham, M. A.; Peng, C. Y.; Nanayakkara, A.; Gonzalez, C.; Challacombe, M.; Gill, P. M. W.; Johnson, B. G.; Chen, W.; Wong, M. W.; Andres, J. L.; Head-Gordon, M.; Replogle, E. S.; Pople, J. A. *Gaussian 98*, revision A.7; Gaussian, Inc.: Pittsburgh, PA, 1998.

(34) Becke, A. D. *Phys. Rev. A* **1988**, *38*, 3098−3100.

(35) Becke, A. D. *J. Chem. Phys.* **1993**, *98*, 5648−5652.

(36) Lee, C.; Yang, W.; Parr, R. G. *Phys. Rev. B* **1988**, *37*, 785−789.

(37) Stevens, P. J.; Devlin, F. J.; Chabalowski, C. F.; Frisch, M. J. *J. Phys. Chem.* **1994**, *98*, 11623−11627.

(38) Schlegel, H. B. *J. Comput. Chem.* **1982**, *3*, 214−218.

(39) Schlegel, H. B. *Adv. Chem. Phys.* **1987**, *67* (Pt. 1), 249−286.

(40) Schlegel, H. B., Yarkony, D. R., Eds.; World Scientific: Singapore, 1995; p 459.

(41) Hay, P. J.; Wadt, W. R. *J. Chem. Phys.* **1985**, *82*, 270−283.

(42) Wadt, W. R.; Hay, P. J. *J. Chem. Phys.* **1985**, *82*, 284−298.

(43) Hay, P. J.; Wadt, W. R. *J. Chem. Phys.* **1985**, *82*, 299−310.

(44) Scott, A. P.; Radom, L. *J. Phys. Chem.* **1996**, *100*, 16502−16513.

(45) Wong, M. W. *Chem. Phys. Lett.* **1996**, *256*, 391−399.

(46) Bach, R. D.; Dmitrenko, O.; Glukhovtsev, M. N. *J. Am. Chem. Soc.* **2001**, *123*, 7134−7145.